

Mixing Mechanism of a Discrete Co-Flow Jet Airfoil

Bertrand P. E. Dano, Alexis Lefebvre and Gecheng Zha
University of Miami, Coral Gables, FL 33124, USA

Abstract: The flow mechanism leading to the enhanced performance of a discrete co-flow jet (dCFJ) airfoil is investigated. Flow visualization and DPIV are used to analyze the difference between the flow along discrete jets and over the tabs used for discretization of the slot jet. Results show that the entrainment is uniform over the leading jet as long as the tab size is small enough. The jets expand spanwise, inducing downward momentum toward the surface of the airfoil. Combined with the momentum increase due to the CFJ, the dCFJ is shown to dramatically increase lift up to 150% from the baseline airfoil and delay separation up to 10° angle of attack. More results and analysis will be presented in the final paper.

Nomenclature

| | |
|-----------|--|
| AoA | Angle of attack |
| C | Chord length |
| CFJ | Co-flow jet |
| CC | Circulation control |
| C_L | Lift coefficient |
| C_D | Drag coefficient |
| C_μ | Jet momentum coefficient |
| D | Drag |
| L | Lift |
| M | Mach number |
| OF | Obstruction factor |
| p | Static pressure |
| P_t | Total pressure |
| Re | Reynolds number |
| S | Wing span area |
| \dot{m} | Jet mass flow rate |
| u,v,w | Velocity components in x-, y-, and z-direction |
| V | Velocity vector |
| x,y,z | Chord, normal and spanwise directions, with respect to the airfoil |

Subscripts:

| | |
|----------|------------|
| ∞ | Freestream |
| j | Jet |

Greek Letters:

| | |
|----------|---|
| γ | Ratio of specific heats |
| ρ | Density |
| α | Angle of attack |
| β | Angle between slot surface and the line normal to chord |

I. Introduction

Over the past decade, a large number of flow control techniques for airfoil performance enhancement have shown breakthroughs from conventional aerodynamic constraints and achieves drastic performance enhancement [1, 2, 3, 4, 5, 6, 7]. Various flow control techniques have been pursued recently including zero-net mass flux (ZNMF) synthetic jets [8, 9, 10] using acoustic wave excitation and dielectric-barrier discharge plasma actuators [11, 12]. In recent years, pulsed fluidic actuators are beginning to deliver effective mixing and performance enhancement for realistic high Reynolds number flows [13, 14]. Finally, circulation control (CC) [15, 16] airfoils driven by fluidic actuators have shown steady increasing aircraft performances over the past three decades [17, 18, 19]. The key idea behind all flow control technology (passive or active) is to increase lift and stall margin, and reduce drag with low energy expenditure and minimal solid structure device. The latter aspect imposes weight penalty, system complication, and parasite drag when not in use.

Among all these new techniques, the co-flow jet (CFJ) technology, developed by Zha et al. has shown significant performance enhancement with low energy expenditure[20-23]. Based of fluidic actuators generating simultaneous blowing at the leading edge (LE) and suction near the trailing edge (TE), zero net mass flux (ZNMF) is achieved over the extrado of the airfoil. Performance enhancement was shown to reach up to over 100% increase in lift with negative drag generated at the same time. The implementation of CFJ technology on an actual airplane can be obtained by using pressurized air from the aircraft engines to supply the jet injection, while the air intake of the engines creates the suction. Most recently, Dano and Zha [24] showed that the CFJ performance can be further increased by using discrete jets instead of a single large open slot. Results for various obstruction factors while keeping the same ZNMF showed that CFJ performance can be further increased by using discrete jets instead of a single large open slot. Results for various obstruction factor while keeping the same ZNMF showed that, for increasing obstruction, CL performance increase another 50% while CD decrease to negative values all the way to $AoA=20^\circ$, effectively converting into thrust. For the same obstruction factor, the performance is more enhanced with smaller jet-to jet separation distance.

The purpose of this research is to study the discrete co-flow jet mixing mechanism that allows the additional increase in performance over the original CFJ. The structure of the adjacent jets and the flow over the obstruction are measured and analyzed.

II. Experiment setup and analysis

Wind Tunnel Setup

A NACA 6415 airfoil was used as the baseline airfoil. A schematic of a CFJ airfoil is shown in Fig. 1. A high energy jet is injected near the LE in the direction tangent to the main flow and the same amount of mass flow is drawn into the airfoil near the TE. Pressurized air is injected in a spanwise long cavity near the LE then exits through the spanwise long rectangular slot. A Duocel high density aluminum foam was placed between the inlet and the exit slot to equilibrate the pressure and ensure a uniform exit velocity. Similarly, a spanwise long cavity placed near the TE is used to let the air settle down before being sucked through three suction ports. The injection and suction slot height were 2.00mm and 4.30mm, respectively. All airflow and aerodynamic variables were acquired at the University of Miami 24"x24" wind tunnel facilities. The injection and suction flow conditions were independently controlled. All wind tunnel freestream, CFJ airflow and aerodynamic variables were recorded using a state-of-the-art Labview™ data acquisition system. LE trip was not implemented. Various laser flow visualization techniques were used to monitor the circulation over the upper surface. A LaVision Digital Particle Image Velocimetry (DPIV) system with a Litron Nano Nd:YAG 200 mJ/pulse was used to monitor and acquire the velocity field surrounding the airfoil. A seeder apparatus was used at the inlet of the wind tunnel to seed uniformly the field of view for DPIV acquisition. A high concentration of seeds was injected, effectively showing flow streamlines. An adaptive 64x64 to 32x32 pixels cross-correlation analysis method was used, resulting in a 150x200 vectors (including the airfoil which was masked). A series of 200 instantaneous velocity fields were acquired for each AoA and various mass flow rates.




Discrete CFJ parameters

The range of AoA varied between 0° to 35°. Nominal free stream velocity was $V_\infty = 10$ m/s for all tests and the chord Reynolds number was about 195,000. Similarly to C_L and C_D , the jet momentum coefficient C_μ was defined as follows:

$$C_\mu = \frac{\dot{m} V_j}{\frac{1}{2} \rho_\infty V_\infty^2 S} \quad (1)$$

where \dot{m} is the mass flow rate, V_{jet} is the jet velocity, ρ_∞ is the free stream density, V_∞ is the free stream velocity, and S is the span area of the airfoil. As the obstruction factors (OF) is increased, the jet exit area is reduced, which in turns increases the jet exit velocity. Therefore, one can see from equation (1) that, for a same mass flow rate, C_μ will change between tests and consequently, the mass flow rate will be used for cases comparison. For a given OF, a large number of combinations can be obtained depending on the number of tabs and desired tab and jet width. Table 1 shows the list of the three cases presented in this paper. Priority was given to configuration containing the larger (hereafter labeled A) and smaller number of discrete jets (hereafter labeled B). A close-up photo of discrete tabs in place is shown in Fig. 2. The baseline test for comparison will be the open slot CFJ (OCFJ) i.e. OF=0 Mass flow rates of $\dot{m}=0$ kg/s, 0.030 kg/s, 0.045 kg/s and 0.060 kg/s (hereafter called M0, M1, M2 and M3) are used. The corresponding OCFJ jet momentum coefficients are $C_\mu=0, 0.08, 0.15$ and 0.26 .

Table 1. Matrix of discrete CFJ configuration

| Config. name | Obstruction Factor | Nb of tabs | Tab width (mm) | Jet width (mm) | Schematic representation |
|--------------|--------------------|------------|----------------|----------------|---|
| OCFJ | 0 | 0 | 0 | 304.8 |  |
| dCFJ 2/3 | 2/3 | 20 | 10.16 | 1.036 |  |
| dCFJ 3/4 | 3/4 | 15 | 15.24 | 1.0546 |  |

III. Results

Aerodynamic Performance

Lift coefficient C_L and drag coefficient C_D for the baseline, OCFJ and three different dCFJ, already presented in [24], are shown in Fig. 3. These results are for M3=0.060 kg/s. One can see that, the OCFJ provides a 50% to 100% increase in lift and noticeably decreases the drag. When dCFJ is used, with the same ZNMF, lift is further increased by another 20% to 50% while drag is similarly reduced and becomes thrust all the way up to AoA=25-30°. Stall angle for baseline was $AoA_{Stall} \sim 23^\circ$. With OCFJ, AoA_{Stall} was delayed by 5°. With dCFJ, AoA_{Stall} is delayed by up to 10°. Overall the use of discrete jets significantly improves the performance of the CFJ technology and leads to important reductions in energy expenditure.

Flow Visualization and PIV results

The above results demonstrate that better performance can be obtained by increasing the OF. For a given OF, better results were systematically obtained for higher number of discrete jets [24]. Preliminary flow visualizations and 2D DPIV were obtained to understand the flow mechanism. Fig. 4 and Fig. 5 show

the air flow at $AoA=25^\circ$ with the CFJ turned off and the corresponding average velocity field, respectively. One can see that the flow is largely separated. Air flows along the airfoil in the upstream direction from the TE to the LE. A series of large clockwise (CW) vortical rollups are observed developing from the separation point flowing down the shear layer.

Fig. 6 and Fig. 7 show the air flow for $AoA=15^\circ$ with $\dot{m}=0.06\text{kg/s}$ along the symmetry plan of a discrete jet and over a tab, respectively. Note, the discrete jets were not seeded. For the jet, series of counter-clockwise (CCW) vortices are observed as the jet shear layer develops. The flow over the tab doesn't appear to create any disturbance, but unsteady patches of unseeded air can be observed further downstream (see yellow arrow in Fig. 7). This demonstrates that the jet is expanding in the spanwise direction, effectively increasing the mixing downstream of the tabs. Fig. 8 and Fig. 9 show the corresponding average velocity fields. For the flow over the jet, air is entrained over the LE and mixes with the jet. For the flow over the tab, air is also entrained over the LE. Velocity decreases slightly past the tab, but increases once again as the jet spreads spanwise in the tab flow plan. No disparity in velocity magnitude is detected in the LE area, showing that adjacent discrete jets are efficiently accelerating the air uniformly over the entire LE.

Fig. 10 and Fig. 11 show the average velocity fields for dCFJ 2/3 (Table 1) at $AoA=25^\circ$ and $\dot{m}=0.060\text{kg/s}$. In comparison, to Fig. 5, the flow remains attached with a large accelerated flow over the entire airfoil. Similar results to $AoA=15^\circ$ are observed with jet incursion in the tab flow plan at the same location. Fig. 12 and Fig. 13 show the average velocity fields for dCFJ 3/4 (Table 1) at $AoA=25^\circ$ and $\dot{m}=0.060\text{kg/s}$. Increasing the obstruction clearly increase the overall velocity magnitude: higher velocities are observed over the entire LE. The jet incursion in the tab plan becomes visible at the tab area which comes as a surprise since the tab width is increased for dCFJ 3/4 (Table 1). Thus, the jet entrainment is believed to spread spanwise, effectively compensating for the velocity deficit in the tab plan. Investigation of the streamline alignment with the airfoil profile, as shown in Fig. 14, shows that the jet flow progressively separates from the surface while the tab flow is pulled down toward the surface. These results suggest that the tab flow becomes more efficient at reducing flow separation.

While it is evident that the flow structure is three-dimensional, the span velocity magnitude is only a fraction of the jet and streamwise velocity. Stereo-PIV needs to be implemented for complete assessment of the flow dynamics. However, these preliminary 2D-PIV results give a reasonable picture of the mechanism leading to the dCFJ aerodynamics enhancements.

Work in Progress

The following work is in progress and will be reported in the final paper:

- 1) Stereo-PIV and 3D-velocity volume rendering of the flow field and streamlines to interpret the jet-to-tab flow spanwise interaction.
- 2) Vortex detection algorithm (VDA) methods and Proper Orthogonal Analysis will be used to analyze the vortical structure

REFERENCES

- [1] W. L. I. Sellers, B. A. Singer, and L. D. Leavitt, "Aerodynamics for Revolutionary Air Vehicles." AIAA 2004-3785, June 2003.
- [2] M. Gad-el Hak, "Flow Control: The Future," Journal of Aircraft, vol. 38, pp. 402–418, 2001.
- [3] M. Gad-el Hak, Flow Control, Passive, Active, and Reactive Flow Management. Cambridge University Press, 2000.
- [4] S. Anders, W. L. Sellers, and A. Washburn, "Active Flow Control Activities at NASA Langley." AIAA 2004-2623, June 2004.
- [5] C. P. Tilmann, R. L. Kimmel, G. Addington, and J. H. Myatt, "Flow Control Research and Application at the AFRL's Air Vehicles Directorate." AIAA 2004-2622, June 2004.
- [6] D. Miller, , and G. Addington, "Aerodynamic Flowfield Control Technologies for Highly Integrated Airframe Propulsion Flowpaths." AIAA 2004-2625, June 2004.
- [7] V. Kibens and W. W. Bower, "An Overview of Active Flow Control Applications at The Boeing Company." AIAA 2004-2624, June 2004.
- [8] R. Holman, Y. Utturkar, R. Mittal, and L. Cattafesta, "Formation Criterion for Synthetic Jets," AIAA Journal, vol. 43, No. 10, pp. 2110–2116, 2005.
- [9] A. Glezer and M. Amitay, "Synthetic Jets," Annual Review of Fluid Mechanics, vol. 24, 2002.
- [10] Crittenden, T. and Glezer, A., "A High-Speed Compressible Synthetic Jet," Physics of Fluids, vol. 18, 1, p. 017107, 2006.
- [11] T. C. Corke and M. L. Post, "Overview of Plasma Flow Control: Concepts, Optimization, and Applications." AIAA Paper 2005-0563, Jan. 2005.
- [12] C. Enloe, T. E. McLaughlin, G. I. Font, and J. W. Baughn, "Frequency Effects on the Efficiency of Aerodynamic Plasma Actuator ." AIAA Paper 2006-0166, Jan. 2006.
- [13] Raman, G. , "Using controlled unsteady fluid mass addition to enhance jet mixing. ," AIAA Journal, vol. 35, No. 4, pp. 647–656, 1997.
- [14] Freund, J.B. and Moin, P. , "Jet mixing enhancement by high-amplitude fluidic actuation," AIAA Journal, vol. 38, No. 10, pp. 1863–1870, 2000.
- [15] N. Wood and J. Nielsen, "Circulation Control Airfoils-Past, Present, Future." AIAA Paper 85-0204, 1985.
- [16] R. J. Englar, "Circulation Control Pneumatic Aerodynamics: Blown Force and Moment Augmentation and Modifications; Past, Present and Future." AIAA 2000-2541, June 2000.
- [17] M. Wilson and C. von Kerczek, "An Inventory of Some Force Procedure for Use in Marine Vehicle Control." DTNSRDC-791097, Nov, 1979.
- [18] G. S. Jones, "Pneumatic Flap Performance for a 2D Circulation Control Airfoil, Steady & Pulsed." Applications of Circulation Control Technologies, Chapter 7, p. 191-244, Vol. 214, Progress in Astronautics and Aeronautics, AIAA Book Series, Editors: Joslin, R. D. and Jones, G. S., 2006.

- [19] G.-C. Zha, W. Gao, and C. Paxton, "Jet Effects on Co-Flow Jet Airfoil Performance," AIAA Journal, No. 6, vol. 45, pp. 1222–1231, 2007.
- [20] G.-C. Zha and D. C. Paxton, "A Novel Flow Control Method for Airfoil Performance Enhancement Using Co-Flow Jet." Applications of Circulation Control Technologies, Chapter 10, p. 293-314, Vol. 214, Progress in Astronautics and Aeronautics, AIAA Book Series, Editors: Joslin, R. D. and Jones, G.S., 2006.
- [21] G.-C. Zha, C. Paxton, A. Conley, A. Wells, and B. Carroll, "Effect of Injection Slot Size on High Performance Co-Flow Jet Airfoil," AIAA Journal of Aircraft, vol. 43, 2006.
- [22] G.-C. Zha, B. Carroll, C. Paxton, A. Conley, and A. Wells, "High Performance Airfoil with Co-Flow Jet Flow Control," AIAA Journal, vol. 45, 2007.
- [23] Dano, D. Kirk, and G.-C. Zha, "Experimental Investigation of Jet Mixing Mechanism of Co- Flow Jet Airfoil", [AIAA-2010-4421](#), 5th AIAA Flow Control Conference, 28 Jun - 1 Jul 2010, Chicago, IL
- [24] B. P. E. Dano, G.-C. Zha, M. Castillo, and P. Ly, "Experimental Study of Co-Flow Jet Airfoil Performance Enhancement Using Micro Discreet Jets." Proceedings of 49th AIAA Aerospace Sciences Meeting, Orlando, FL, 4-7 January 2011.

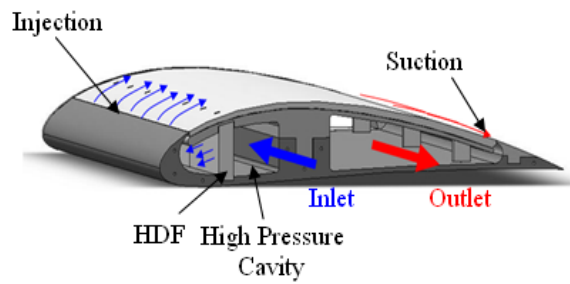


Fig.1 Schematic and concept of CFJ airfoil.



Fig. 2 Picture of the tabs in position (dCFJ 2/3).

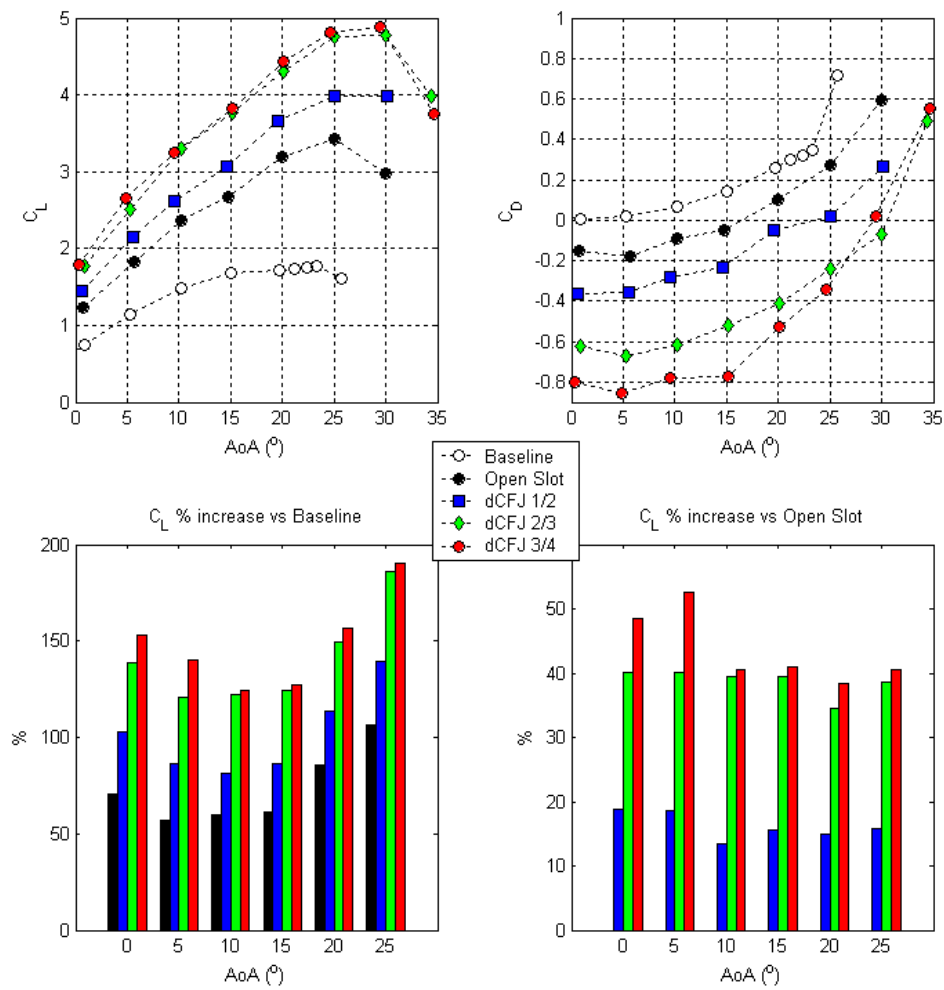


Fig. 3 Overall Performance enhancement for various obstruction factors at $M=0.060$ kg/s.

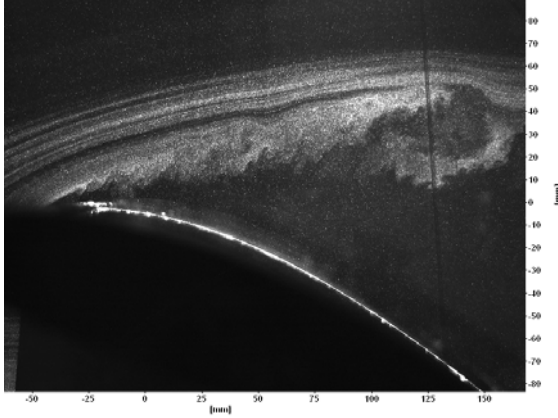


Fig. 4 Flow visualization along a discrete jet (CFJ off, $AoA=25^\circ$).

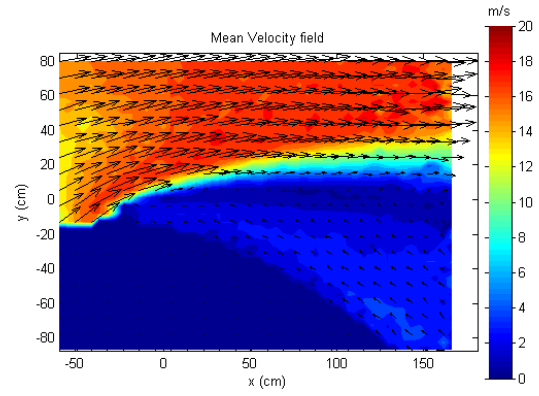


Fig. 5 Average velocity field (CFJ off, $AoA=25^\circ$).

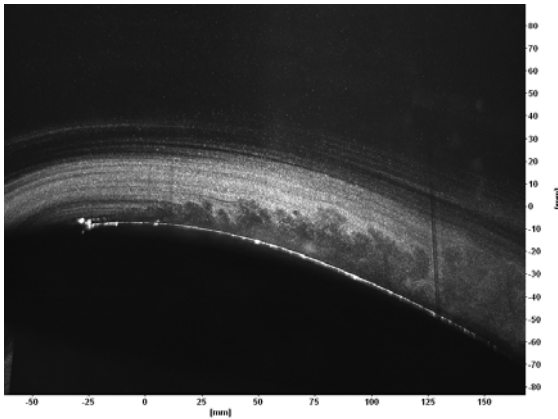


Fig. 6 Flow visualization along a jet ($AoA=15^\circ$ and $\dot{m}=0.060\text{kg/s}$).

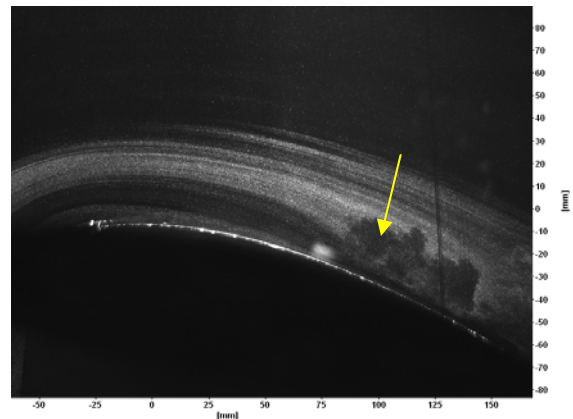


Fig. 7 Flow visualization over a tab ($AoA=15^\circ$ and $\dot{m}=0.060\text{kg/s}$).

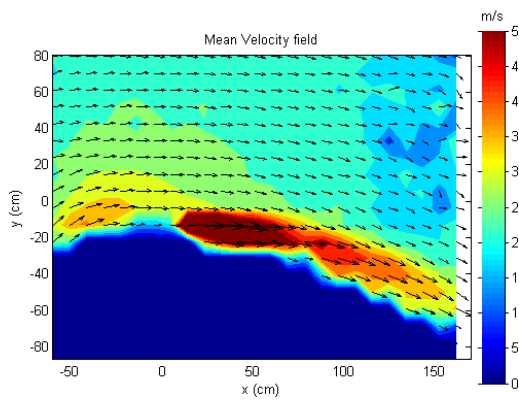


Fig. 8 Average velocity field along a discrete jet (dCFJ 2/3, $AoA=15^\circ$ and $\dot{m}=0.060\text{kg/s}$).

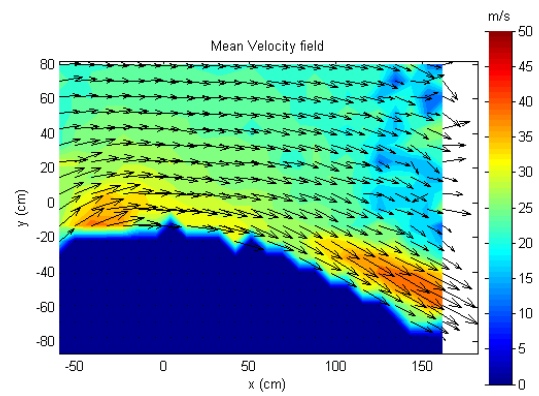


Fig. 9 Average velocity field over a tab (dCFJ 2/3, $AoA=15^\circ$ and $\dot{m}=0.060\text{kg/s}$).

